9276–9288 *Nucleic Acids Research, 2018, Vol. 46, No. 18* *Published online 7 September 2018*
doi: 10.1093/nar/gky803

Signaling specificity in the c-di-GMP-dependent network regulating antibiotic synthesis in *Lysobacter*

Gaoge Xu[1,2], Sen Han[1], Cuimei Huo[1], Ko-Hsin Chin[3], Shan-Ho Chou[3], Mark Gomelsky[4], Guoliang Qian[1,*] and Fengquan Liu[2,*]

[1]College of Plant Protection, Nanjing Agricultural University, Nanjing 210095, China/Key Laboratory of Integrated Management of Crop Diseases and Pests (Nanjing Agricultural University), Ministry of Education, Nanjing 210014, P.R. China, [2]Institute of Plant Protection, Jiangsu Academy of Agricultural Sciences, Nanjing 210014, P.R. China, [3]Institute of Biochemistry, and NCHU Agricultural Biotechnology Center, National Chung Hsing University, Taichung, Taiwan, ROC and [4]Department of Molecular Biology, University of Wyoming, Laramie, Wyoming 82071, USA

Received May 03, 2018; Revised August 25, 2018; Editorial Decision August 27, 2018; Accepted August 28, 2018

ABSTRACT

Enzymes controlling intracellular second messengers in bacteria, such as c-di-GMP, often affect some but not other targets. How such specificity is achieved is understood only partially. Here, we present a novel mechanism that enables specific c-di-GMP-dependent inhibition of the antifungal antibiotic production. Expression of the biosynthesis operon for Heat-Stable Antifungal Factor, HSAF, in *Lysobacter enzymogenes* occurs when the transcription activator Clp binds to two upstream sites. At high c-di-GMP levels, Clp binding to the lower-affinity site is compromised, which is sufficient to decrease gene expression. We identified a weak c-di-GMP phosphodiesterase, LchP, that plays a disproportionately high role in HSAF synthesis due to its ability to bind Clp. Further, Clp binding stimulates phosphodiesterase activity of LchP. An observation of a signaling complex formed by a c-di-GMP phosphodiesterase and a c-di-GMP-binding transcription factor lends support to the emerging paradigm that such signaling complexes are common in bacteria, and that bacteria and eukaryotes employ similar solutions to the specificity problem in second messenger-based signaling systems.

INTRODUCTION

Cyclic dimeric GMP, c-di-GMP (1), is a ubiquitous dinucleotide second messenger in diverse bacteria. It controls multiple physiological processes via intracellular protein effectors (or receptors) and riboswitches. Among the best-characterized processes are changes in bacterial planktonic and biofilm lifestyles, pathogenicity, cell cycle and differentiation (2,3). C-di-GMP is synthesized via the condensation of two GTP molecules by diguanylate cyclases, DGCs, which possess the characteristic GGDEF catalytic domain (4,5). C-di-GMP is hydrolyzed primarily by specific phosphodiesterases, PDEs, that contain either EAL (6–8) or HD-GYP (9) catalytic domains. Bacterial genomes often encode numerous DGC and PDE proteins. If these enzymes were to regulate c-di-GMP-dependent targets indiscriminately, it could result in an unmanageable cacophony of responses. The question of how activation of certain enzymes involved in c-di-GMP synthesis and hydrolysis results in specific outcomes has emerged early on (10), and several answers to this question have emerged over the years (2,3). In this study, we describe a novel mechanism ensuring signaling specificity that involves an interaction between a PDE and a c-di-GMP-binding transcription factor in *Lysobacter enzymogenes*.

Lysobacter enzymogenes is a nonpathogenic, plant-associated gammaproteobacterium known for synthesis of the antifungal antibiotic Heat-Stable Antifungal Factor, HSAF (11–14), which makes it an attractive biological control agent for fungal diseases of agriculturally important plants (11,12,15). Therefore, identifying genes and growth conditions that regulate HSAF production has been of significant interest (16,17). Our earlier work revealed that elevated intracellular c-di-GMP levels are detrimental for HSAF production due to lower HSAF biosynthesis gene expression (18). It is noteworthy that biosynthesis of antibiotics and other secondary metabolites is emerging as a common target of c-di-GMP-dependent regulation in bacteria (19). The first example of the regulation of antibiotic production by c-di-GMP was described in *Serratia,* in which PigX, a GGDEF-EAL domain protein might function as a PDE to repress prodigiosin (Pig) production by controlling transcription of the Pig biosynthetic operon (20). Additional examples of such regulation include acti-

*To whom correspondence should be addressed. Tel: +86 25 84396109; Fax: +86 25 84396109; Email: glqian@njau.edu.cn
Correspondence may also be addressed to Fengquan Liu. Tel: +86 25 84390277; Fax: +86 25 84390277; Email: fqliu20011@sina.com

nomycetes, *Streptomyces coelicor* and *S. venezuelae*, where c-di-GMP inhibits synthesis of several antibiotics, i.e. actinorhodin, undecylprodigiosin, and methylenomycin. Inhibition of expression of antibiotic biosynthesis genes in these species is mediated by the c-di-GMP-binding repressor BldD (21). In yet another actinomycete, *Saccharopolyspora erythraea*, a BldD homolog regulates the synthesis of the antibiotic erythromycin (22). In the gammaproteobacterium, *Pseudomonas aeruginosa*, high intracellular c-di-GMP levels promote synthesis of the antibiotic phenazine pyocyanin (23), while in the alphaproteobacterium *Ruegeria mobilis*, c-di-GMP inhibits production of the antibiotic tropodithietic acid (24).

Our earlier studies into the mechanisms of c-di-GMP-dependent regulation of HSAF gene expression in *L. enzymogenes* revealed two major components, the HD-GYP domain PDE, RpfG, and the c-di-GMP-binding transcription factor, Clp (25,26). From the studies of Clp proteins in bacteria of genus *Xanthomonas*, which is related to *Lysobacter*, we know that the DNA-binding affinity of Clp is inhibited by c-di-GMP (27–29). In this work, we characterized the role of *L. enzymogenes* Clp in regulating HSAF biosynthesis gene expression in a c-di-GMP dependent manner.

To identify additional c-di-GMP components affecting HSAF synthesis, we screened all putative PDEs in *L. enzymogenes* and uncovered yet another PDE, hereby designated LchP (*Lysobacter* c-di-GMP and HSAF-associated Phosphodiesterase) that plays a disproportionately high role in regulating HSAF production despite its low PDE activity. The impact of LchP is magnified due to its ability to form a complex with Clp, which enhances the PDE activity of LchP. We expect that the phenomenon where c-di-GMP effector proteins form complexes with specific PDEs is not limited to the *L. enzymogenes* LchP-Clp system. Instead, it likely represents a common mechanism that helps establishing signaling specificity in bacteria possessing multicomponent second messenger networks.

MATERIALS AND METHODS

Bacterial strains, plasmids and growth conditions

Strains and plasmids used in this study are listed in Supplementary Table S1. *Escherichia coli* was grown in Lysogenic broth (LB) at 37°C with appropriate antibiotics. Unless stated otherwise, *L. enzymogenes* was grown in LB medium at 28°C with appropriate antibiotics—kanamycin (Km), 25 μg/ml, for mutant construction and gentamicin (Gm), 150 μg/ml, for plasmid maintenance.

Bioinformatics analysis

The EAL and HD-GYP domain-containing proteins in *L. enzymogenes* strain OH11 were identified with the help of Pfam 30.0 database (30). Briefly, the HMM model domains of the EAL (PF00563) and HD-GYP (PF01966) domains were downloaded and used to screen (via BLASTP) of the complete genome of *L. enzymogenes* OH11 (13) using the HMMER software (31).

Genetic methods

The in-frame deletions in *L. enzymogenes* OH11 were generated via double-crossover homologous recombination as described previously (32) using primers listed in Supplementary Table S2. In brief, the flanking regions of each gene were PCR-amplified and cloned into the suicide vector pEX18Gm (Supplementary Table S1). The deletion constructs were transformed into the wild-type strain by electroporation. The single-crossover recombinants were selected on LB plates supplemented with Km and Gm. The recombinants were cultured in LB without antibiotics for 6 h and subsequently plated on LB agar containing 10% (w/v) sucrose and Km. The sucrose-resistant, Km-resistant but Gm-sensitive colonies representing double crossovers were picked up. In-frame gene, deletions were verified by PCR using appropriate primers (Supplementary Table S2).

Gene complementation constructs were generated as described earlier (33). In brief, DNA fragments containing the full-length genes along with their promoters were PCR-amplified and cloned into the broad-host vector pBBR1-MCS5 (Supplementary Table S1). The plasmids were transformed into the wild-type strain by electroporation, and the transformants were selected on the LB plates containing Gm.

The DNA containing PA and PB sites, as well as their derivatives (PA_{sm} and PB_{sm}) were synthesized by GENEWIZ (Suzhou, China). The PA_{sm} and PB_{sm} were used to replace the native PA and PB sequences in the *L. enzymogenes* chromosome via double-crossover homologous recombination, as described above.

Quantitative RT-PCR, qRT-PCR

Cells were grown in 1/10 Tryptic Soy Broth (TSB) and collected at OD_{600}, 1.5. RNA was extracted using a Bacterial RNA Kit (OMEGA, China) according to the manufacturer's protocol. RNA concentrations were measured by a Nanodrop Spectrophotometer ND-1000 UV (Thermo Fisher, USA). 500 ng RNA from each sample was used to generate total cDNA by using the PrimeScript RT reagent Kit with gDNA Eraser (Takara, Japan). Primers were listed in the revised Supplementary Table S2. qRT-PCR was carried out using an Applied Biosystems 7500 system. The *16S rRNA* gene was used as an internal control, as described earlier (25,33). Each PCR tube (20 μl) contained 10 μl 2× SYBR Premix Ex·taq (Takara, Japan), 2 × 0.4 μl primer, 0.4 μl Rox dye II (Takara, Japan), 2 μl cDNA and 6.8 μl water. The cycling protocol was: 95°C for 30 s, 40 cycles of 95°C for 5 s, 60°C for 34 s, before fluorescence detection. A melting curve was determined using 1 cycle of 95°C for 15 s, 60°C for 60 s and 95°C for 30 s. Data were analyzed by Applied Biosystems 7500 software v2.0.6. Amplification specificity was assessed by melting curve analysis. Relative fold change of the expression of individual genes was calculated using the $2^{-\Delta\Delta Ct}$ method (34).

E. coli reporter assays for evaluating DGC and PDE activities

The *E. coli* motility-based assays of DGC or PDE activities have been described earlier (35,36). Briefly, the con-

structs expressing various fragments of LchP were cloned into the vector pBAD/Myc-His B (Supplementary Table S1) and transformed into *E. coli* MG1655 and MG1655 *yhjH* mutant. The transformed *E. coli* strains were grown in LB overnight, and 2 μl of cultures was spotted onto soft (0.25%) agar plates containing 1% tryptone, 0.5% NaCl and 0.1% arabinose. Diameters of the swimming zones were assessed after a 6-h incubation at 37°C. Three biological replicates were run, where each strain was plated in five replicates.

Protein overexpression and purification

The DNA corresponding to the cytoplasmic fragment of LchP, LchP-PGE, was amplified by PCR using primers listed in Supplementary Table S2 and cloned into vector pMAL-p2x to generate the MBP-LchP-PGE protein fusion. The resulting plasmid was transformed into *E. coli* BL21(DE3) (Supplementary Table S1) for protein expression and purification. 2 mL of the overnight culture was transferred into 200 ml fresh LB at 37°C and grown with shaking (200 rpm) until OD_{600}, 0.6. Subsequently, isopropyl β-D-1-thiogalactopyranoside (IPTG, Sigma, USA), was added to achieve the final concentration of 0.5 mM. The culture was incubated for additional 4 h at 28°C. Cells were collected by centrifugation (13 000 rpm) at 4°C, resuspended in 25 ml phosphate buffer saline (PBS) lysis buffer containing 10 mM protease inhibitor (PMSF, Sigma, USA), followed by a 20 min sonication using Sonifier 250 (Branson Digital Sonifier, Branson). The crude cell extracts were separated at 13 000 rpm at 4°C for 30 min. The supernatant was passed through 1 ml amylose resin (New England Biolabs) that retained the MBP-LchP-PGE protein. The column was washed with 200 ml of PBS buffer, and subsequently 30 ml 10 mM maltose elution buffer for protein elution. Protein purity was assessed by SDS-PAGE and protein concentration was determined using BCA assay kit (Sangon Biotech).

The DNA corresponding to RpfG was amplified by PCR using primers listed in Supplementary Table S2 and cloned into vector pET30a to generate the RpfG-His protein fusion. The resulting plasmid was transformed into *E. coli* BL21(DE3) (Supplementary Table S1) for protein expression and purification. The method used for purification of RpfG-His protein is the same with that of MBP-LchP-PGE protein, except using the Ni-NTA beads (Yeasen company, China) and 250 mM imidazole solution as elution buffer instead of amylose resin and 10 mM maltose elution buffer respectively.

DGC and PDE activity assays *in vitro*

The PDE activity assay was performed essentially as described earlier (6). Briefly, 2 μM LchP-PGE-MBP or its derivatives were tested in buffer containing 60 mM Tris–HCl (pH 7.6), 50 mM NaCl, 10 mM $MnCl_2$ and 10 mM $MgCl_2$. The reaction was started by the addition of 100 μM c-di-GMP. The DGC activity assay was performed essentially as described earlier (5). Briefly, 2 μM LchP-PGE-MBP or its derivatives were tested in buffer containing 75 mM Tris–HCl (pH 8.0), 250 mM NaCl, 25 mM KCl, 10 mM $MgCl_2$. The reaction was started by the addition of 100 μM GTP. All reaction mixtures were incubated at 37°C for 8 or 10 h, followed by boiling for 10 min to stop the reaction. The samples were filtered through a 0.2-μM pore size cellulose-acetate filter, and 20 μl of each sample was loaded onto a reverse-phase C18 column, separated by HPLC. The separation protocol involved two mobile phases, 100 mM KH_2PO_4 plus 4 mM tetrabutylammonium sulfate (A) and 75% A + 25% methanol (B), as described earlier (5).

HSAF extraction and quantification

HSAF was extracted from 25 ml *L. enzymogenes* cultures grown in 1/10 TSB for 24 h at 28°C with shaking (at 200 rpm). HSAF was detected via HPLC and quantified per unit of OD_{600} as described earlier (12,25,37). Three biological replicates were used, and each was done in three technical replicates.

B2H assay

BacterioMatch II Two-Hybrid system (Agilent Technologies, USA) was used to determine potential interactions between two proteins. The coding regions of target proteins were cloned into pBT and pTGR plasmids and transformed into *E. coli* XL1-Blue MRF′ Kan. If the bait and target proteins interact, the transcription of the *his3* reporter gene is activated resulting in the production of imidazoleglycerol-phosphate dehydratase, which enables colony growth in the presence of the competitive enzyme inhibitor, 3-amino-1,2,4-triazole (3-AT). A second reporter gene *aadA* encoding a protein that confers streptomycin (Str) resistance was used to validate positive protein-protein interactions, according to the protocol of the kit manufacturer. Plasmids pBT-GacS and pTRG-GacS were constructed in this work (Supplementary Table S1) to serve as an additional positive control because the cytoplasmic domain of GacS from *P. aeruginosa* is known to form homodimers (38). The transformants containing empty pTRG and pBT vectors were used as a negative control. All co-transformants were spotted onto the selective medium and grown at 28°C for 3–4 days.

Electrophoretic mobility shift assay (EMSA)

The GST-tagged Clp protein was purified according to the recently described protocol (39). EMSA was performed as follows. Biotin labeled probes PA (50 bp) and PB (50 bp), as well as their scrambled consensus sequence variants, PA_{sm} and PB_{sm}, were synthesized by GENEWIZ (Suzhou, China). Probe and protein extract were incubated in the test system for 20 min at room temperature according to the specifications of LightShift® Chemiluminescent EMSA Kit (ThermoFisher, Waltham, USA). The binding mixture was loaded onto the polyacrylamide gel, electrophoresed, transferred to a nylon membrane and crosslinked, as described in the manufacturer protocol. The biotinylated DNA fragments were detected by chemiluminescence using VersaDoc imaging system (Bio-Rad, Philadelphia, USA).

Isothermal titration calorimetry, ITC

Isothermal titration calorimetry experiments were carried out using a ITC_{200} microcalorimeter (MicroCal). A solution of 25 mM Clp-GST dissolved in low salt buffer (20 mM Tris pH 8.0, 80 mM NaCl) was titrated with 20 injections of 2 ml each at 3 min intervals from a 0.5 mM stock solution of c-di-GMP in the same buffer. Heat of binding (ΔH), the stoichiometry of binding (n), and the dissociation constant (K_d) were calculated from plots of the heat released per mol of ligand injected versus the molar ratio of ligand to receptor using the software provided by the vendor.

Microscale thermophoresis assay, MST

Binding of the Clp-GST fusion protein to the HSAF operon promoter (39) was determined by MST using Monolith NT.115 (NanoTemper Technologies, Germany), according to the recently described protocol (16). Briefly, the 50-bp DNA fragments were labeled with 5-carboxy-fluorescein (FAM). A constant concentration (10 μM) of the labeled promoter in the MST buffer (50 mM Tris, pH 7.5, 150 mM NaCl, 10 mM $MgCl_2$, 0.05% Tween 20) was titrated against increasing concentrations of Clp-GST dissolved in ddH_2O. The Clp-GST and LchP-PGE-MBP binding was assessed in a similar manner. Briefly, the Clp-GST protein was labeled with the fluorescent dye NT-647-NHS (NanoTemper Technologies GmbH, Germany) via amine conjugation. A constant concentration (40 μM) of the labeled promoter in the MST buffer was titrated against LchP-PGE-GST (concentration range, 1.2 nM–40 μM). MST premium-coated capillaries (Monolith NT.115 MO-K005, Germany) were used to load the samples into the MST instrument at 25°C using 40% MST power, and 20% LED power. Laser on and off times were set at 30 and 5 s, respectively. Binding of Clp-GST to RpfG-His was also detected by this system with similar test conditions. All experiments were performed in triplicate. Data were analyzed using Nanotemper Analysis software v.1.2.101 (NanoTemper Technologies, Germany).

Pull-down assay

The purified proteins were used to perform the pull-down assay in a reaction system comprising 800 μl PBS buffer, 5 μM (final concentration) of Clp-GST and LchP-PGE-MBP protein or RpfG-His protein, and 50 μl GST resin. All samples were incubated at 4°C overnight. The resin was collected by centrifugation and washed 10 times with PBS containing 1% Triton X-100 to remove non-specifically bound proteins. The GST-beads captured proteins were eluted by boiling in 6× SDS loading dye for 10 min. These samples were subjected to SDS-PAGE and Western blotting. Protein detection involved GST- (ab19256), MBP- (ab49923) and His- (ab18184) specific antibodies from Abcam, UK.

c-di-GMP extraction and quantification

Cultures were grown in 1/10 TSB at 28°C until OD_{600}, 1.5. Cells from 2 ml culture were harvested for protein quantification by the BCA assay (TransGen, China). Cells from 8 mL of culture were used for c-di-GMP extraction using 0.6 M $HClO_4$ and 2.5 M K_2CO_3, as described previously (40,41). The samples were analyzed by liquid chromatography–mass spectrometry (LC–MS) on Agilent 6460 Triple Quad LC/MS, as described previously (40–42).

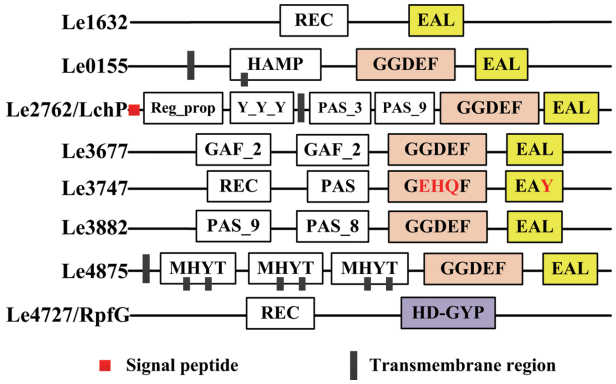

Figure 1. Proteins containing EAL or HD-GYP domains encoded in the *L. enzymogenes* OH11 genome. The GGDEF domains implicated in c-di-GMP synthesis are shown in pink. The EAL and HD-GYP domains implicated in c-di-GMP hydrolysis are shown in yellow and purple, respectively. The residues in the conserved 'GGDEF' and 'EAL' motifs that deviate from the consensuses and therefore likely indicate enzymatically inactive domains, are shown in red. Le4727 is RfpG (26), Le2762 is LchP. Protein domain architectures are from Pfam database (30).

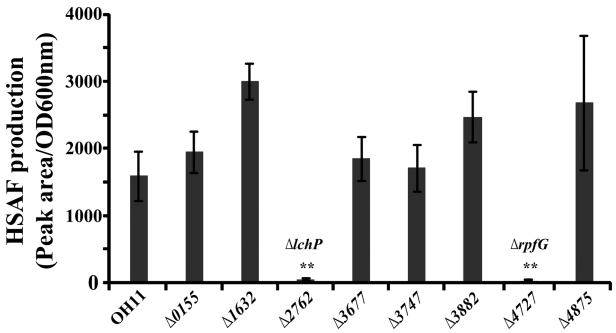

Figure 2. Quantification of HSAF levels produced by the EAL and HD-GYP gene deletion mutants. HSAF was detected by HPLC and quantified as peak area per unit of OD_{600}(16). Δ## indicates deletions in the genes shown in Figure 1.The amounts of HSAF produced by the *lchP* (*Δ2762*) and *rpfG* (*Δ4727*) mutants are lowest among other mutants. Average data from three experiments are presented, ±SD. $^{**}P < 0.01$, relative to the wild-type strain, OH11.

RESULTS

Identification of c-di-GMP PDEs involved in regulating HSAF production in *L. enzymogenes*

The genome of *L. enzymogenes* strain OH11 encodes eight proteins containing GGDEF, EAL or HD-GYP domains (Figure 1). One of these proteins RpfG, is the HD-GYP domain PDE whose inactivation blocks HSAF production (26). To identify additional PDEs involved in HSAF regulation, we made deletions in seven EAL domain encoding genes (Supplementary Table S3) and measured HSAF levels in each of the constructed mutants.

In accord with our earlier findings (26), HSAF production in the *rpfG* mutant was completely suppressed (Figure 2). The mutant in *le2762* (hereby designated *lchP*) had the

second lowest HSAF levels after the *rpfG* mutant (Figure 2). Importantly, the *lchP* mutation did not impair bacterial growth or other readily observable phenotypes (Supplementary Figure S1), thus implying that LchP plays a specific role in regulating HSAF production. To verify that the defect in HSAF production in the *lchP* mutant was due to the lack of LchP, we complemented the mutation with a plasmid-encoded *lchP* gene, and found that the plasmid-encoded *lchP* partially restored HSAF synthesis in the *lchP* mutant (Figure 3A).

RpfG affects HSAF production at the level of gene expression (26), therefore we expected LchP to also affect gene expression. To test this prediction, we measured, via quantitative RT-PCR (qRT-PCR), mRNA levels of *lafB*, the first gene in the HSAF biosynthesis operon (17). We found the level of the *lafB* transcript in the *lchP* mutant to be decreased by >2-fold, compared to the wild type (Figure 3B). Plasmid-encoded *lchP* in partially restored *lafB* gene expression in the *lchP* mutant (Figure 3B). This result confirms that LchP acts at the level of HSAF biosynthesis gene expression but does not preclude additional roles of LchP in regulating HSAF production.

The PDE activity of LchP is important for regulating HSAF biosynthesis gene expression

Based on the fact that both RpfG and LchP upregulated HSAF biosynthesis gene expression, we expected LchP to function as a PDE. Here, we tested this prediction. LchP is a multidomain protein containing a periplasmic sensory domain Reg_prop linked to the Y-Y-Y domain, a transmembrane region followed by two cytoplasmic PAS domains and the GGDEF-EAL domain tandem (Figure 1). Sequence analysis revealed that both the GGDEF and EAL domains contain all residues essential for DGC and PDE activities (2), thus suggesting that LchP may be a bifunctional DGC-PDE enzyme.

We addressed the question of LchP enzymatic activity using several approaches. First, we compared intracellular c-di-GMP concentrations in the *lchP* mutant and the wild type and in the HSAF-production medium (1/10 TSB). We found the concentration in the mutant to be significantly higher (Figure 3C). While this finding was in agreement with the predicted PDE function of LchP, the increase in c-di-GMP concentration was very modest, which was somewhat unexpected given strong inhibition of HSAF production in the *lchP* mutant (Figure 2).

To further investigate enzymatic activity of LchP, we employed *E. coli*-based motility screens where swim zones in the semi-solid agar serve as proxies of intracellular c-di-GMP concentrations (35). In the highly motile, low c-di-GMP strain, MG1655, heterologous DGCs decrease the swim zone sizes (5). Conversely, in the high c-di-GMP strain, MG1655 Δ*yhjH*, that lacks the most potent *E. coli* c-di-GMP PDE, YhjH/PdeH (43,44), heterologous PDEs increase swim zone sizes (5). According to these screens, LchP functions as a DGC, but not PDE (Figure 3D, E and Supplementary Table S4). Finding DGC activity was not surprising given that the GGDEF domain in LchP is intact, however, the lack of PDE activity contradicted the *L. enzymogenes* phenotype. We hypothesized that improper LchP protein folding or the absence of appropriate stimuli in *E. coli* may have accounted for the observed inconsistency. This prompted us to investigate enzymatic activity of the truncated, cytoplasmic fragment of LchP that contains only the PAS+GGDEF+EAL domains (designated LchP-PGE). LchP-PGE exhibited no DGC activity in MG1655 and weak PDE activity in MG1655 Δ*yhjH* (Figure 3D and E).

Finally, we carried out biochemical assays using LchP-PGE purified as a fusion to the maltose binding protein (designated LchP-PGE-MBP) (Supplementary Figure S2). LchP-PGE-MBP hydrolyzed c-di-GMP to 5′-pGpG (Figure 3I), consistent with its PDE activity. When GTP was added as substrate, LchP-PGE-MBP produced c-di-GMP, indicative of its DGC activity, as well as the product of c-di-GMP hydrolysis, 5′-pGpG (Figure 3J). Therefore, according to biochemical assays, LchP is a bifunctional DGC-PDE enzyme.

To better understand the roles of the GGDEF and EAL domains in LchP function, we generated a series of point mutations in the conserved 'GGDEF' and 'EAL' motifs of the GGDEF and EAL domains that are essential for their respective enzymatic activities (2). We found that mutations of the conserved 'EAL' motif (EAL→AAA) completely abolished PDE activity of LchP-PGE, whereas mutations of the conserved 'GGDEF' motif (GGDEF→GGAAF) partially decreased PDE activity (Figure 3E; Supplementary Figure S3). The PAS-GGDEF or PAS-EAL constructs lacked DGC and EAL activities, respectively (Figure 3D and E). The expression levels of the generated mutants were comparable to those of the wild-type proteins, as assessed by Western blotting (Supplemental Figure S4). These data suggest that the GGDEF domain possesses some DGC activity and is required for full PDE activity of LchP.

Next, we decided to correlate observations in *E. coli* with those in *L. enzymogenes*. We found that the cytoplasmic fragment of LchP, LchP-PGE, is more efficient in complementing HSAF production of the *lchP* mutation, compared to the full-length LchP (Figure 3A). This is consistent with higher PDE activity of LchP-PGE, compared to LchP, and is consistent with the motility data in *E. coli*. The 'EAL' motif mutant of LchP-PGE lacking PDE activity failed to complement the *lchP* mutation. We conclude that it is the PDE activity of LchP that is important for regulating HSAF biosynthesis in *L. enzymogenes*. The EAL→AAA mutations in the chromosomal *lchP* gene impaired HSAF synthesis, and so did the GGDEF→GGAAF mutations (Figure 3A), which emphasizes the importance of the GGDEF domain for PDE activity of LchP.

To solidify the conclusion that lower c-di-GMP levels increase HSAF production, we expressed in *L. enzymogenes* a potent heterologous PDE, YhjH/PdeH from *E. coli* (36). In parallel, we expressed a potent DGC, Slr1143 from *Synechocystis* sp. (5). Consistent with our expectations, HSAF production was increased upon expression of a heterologous PDE but not a DGC (Figure 3A). Further, expression of a heterologous DGC in the wild-type strain, OH11, lowered *lafB* transcript levels, compared to the vector control (Figure 3B, OH11(Slr) versus OH11(pBBR)).

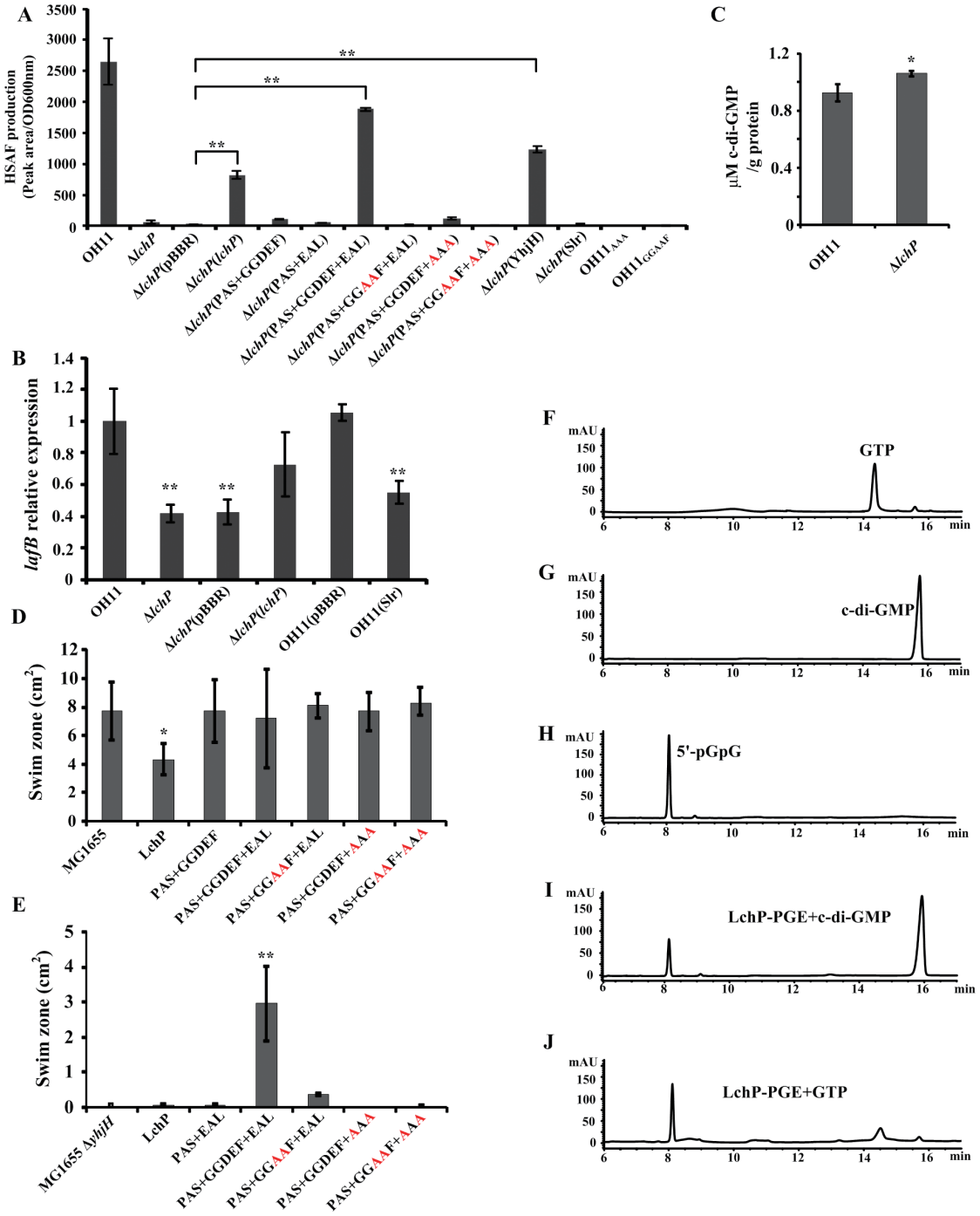

Figure 3. LchP is a bifunctional DGC-PDE enzyme. (**A**) Involvement of the GGDEF and EAL domains in LchP activity. Δ*lchP*(pBBR) and Δ*lchP*(*lchP*) indicate the *lchP* deletion mutant containing empty vector (pBBR1-MCS5) or plasmid *lchP*-pBBR expressing the *lchP* gene, respectively. LchP-PGE is the cytoplasmic fragment of LchP consisting of the PAS+GGDEF+EAL domains. Point mutations in the conserved 'GGDEF' and 'EAL' motifs are shown in red letters. YhjH/PdeH is an active c-di-GMP PDE from *E. coli* (6); Slr (Slr1143) is an active DGC from *Synechocystis* sp. (5). $OH11_{AAA}$, wild type (OH11) containing mutations in the chromosomal *lchP* gene resulting in the EAL→AAA substitution. $OH11_{GGAAF}$, wild type (OH11) containing mutations in the chromosomal *lchP* gene resulting in the GGDEF → GGAAF substitution. Average data from three experiments, ±SD are shown. $^{**}P < 0.01$. (**B**) qRT-PCR analyses of *lafB* mRNA levels in the wild type, OH11, Δ*lchP* mutant and their derivatives. Data from three biological experiments, each done in three technical replicates, +/− SD. The *lafB* mRNA level in the wild type was set as 1. $^{**}P < 0.01$, relative to the wild type. (**C**) Intracellular c-di-GMP concentrations in the wild type and *lchP* mutant showing modestly higher levels in the mutant. Data from three experiments are shown. $^{*}P < 0.05$, relative to the wild type. (**D**) Inhibition of motility in semi-solid agar of strain MG1655 by LchP and its derivatives. Data from three experiments are shown. $^{*}P < 0.05$, relative to MG1655. (**E**) Restoration of swim zones in semi-solid agar in strain MG1655 Δ*yhjH* by LchP and its derivatives. Data of triplicate experiments are shown. $^{**}P < 0.01$, relative to MG1655 Δ*yhjH*. (F–J) Enzymatic activity assays indicating PDE and DGC activities of the cytoplasmic fragment of LchP, LchP-PGE. Standards used in HPLC: GTP (**F**), c-di-GMP (**G**), 5′-pGpG (**H**). 5′-pGpG, a product of c-di-GMP hydrolysis, was detected after incubating LchP-PGE with c-di-GMP (**I**). c-di-GMP and 5′-pGpG, were detected upon incubation of LchP-PGE with GTP (**J**).

Lysobacter Clp is a c-di-GMP-binding factor controlling HSAF biosynthesis gene expression

Here, we turn our attention to the mechanism of c-di-GMP-dependent inhibition of HSAF biosynthesis gene expression. Earlier, we showed that Clp is the major regulator of HSAF biosynthesis gene expression (26,37). *Lysobacter* Clp is approximately 96% similar to the c-di-GMP-binding transcription activator, Clp from *Xanthomonas campestris*, and the residues involved in c-di-GMP binding are conserved between these proteins (Supplementary Figure S5). We therefore anticipated that *L. enzymogenes* Clp mediates c-di-GMP effects on HSAF biosynthesis. To test this hypothesis, we purified the *L. enzymogenes* Clp as GST-fusion via affinity chromatography and examined its ability to bind c-di-GMP by means of Isothermal Titration Calorimetry (ITC). We found that Clp-GST bound c-di-GMP with K_d, 1.5 μM (Figure 4A), which is similar to K_d reported for the *X. campestris* Clp (28).

Next, we tested whether *L. enzymogenes* Clp binds to the upstream region of the HSAF biosynthesis operon. Based on the DNA consensus sequence, 5′-ATGC-N6-GCAT-3′, deciphered for *X. campestris* Clp (45), we identified two potential binding sites of *L. enzymogenes* Clp: 5′-ATCC-N8-GGAT-3′ and 5′-ATCG-N8-CGAT-3′ (Supplementary Figure S6A). To test for Clp binding, we performed an electrophoretic mobility shift assay (EMSA), in which Clp-GST was mixed with a 50-bp DNA probe PA or PB containing either the two binding site. The EMSA assay revealed that Clp binds to both sites (Supplementary Figure S6B and C). Formation of the Clp-PA and Clp-PB protein–DNA complexes can be competitively inhibited by excess of the unlabeled probes (Supplementary Figure S6B and C), suggesting that Clp-DNA interactions are specific. Further, when scrambled DNA sequences, 5′-CGTT-N8-TTGC-3′ (PA_{sm}) and 5′-GGTG-N8-CTGG-3′ (PB_{sm}), were used in the EMSA, Clp showed no binding (Supplementary Figure S6B and C). We conclude that Clp specifically binds to at least two sites in the upstream region of the HSAF biosynthesis operon promoter.

Next, we tested the effect of c-di-GMP on Clp-DNA binding. We found that addition of c-di-GMP at 16 μM caused a readily observable reduction in Clp-PA complex formation, whereas addition of c-di-GMP at lower concentrations caused little or no effect (Figure 4B). Unexpectedly, under the same test conditions, c-di-GMP did not measurably decrease Clp-PB complex formation (Figure 4C). These results suggest that Clp binding to the PA, but not PB site is more sensitive to inhibition by c-di-GMP. To verify this conclusion, we used another technique, Microscale Thermophoresis (MST) (46), to assess Clp binding to the PA and PB sites in the presence or absence of c-di-GMP. First, we measured affinity of Clp to each site. We found that Clp binds PA and PB *in vitro* with K_d, 0.29 μM and 0.08 μM, respectively (Figure 4D and E). Addition of 16 μM c-di-GMP resulted in a ∼4-fold decrease in Clp binding to PA, but no significant change was observed to its binding to PB (Figure 4F and G), in agreement with the EMSA data (Figure 4B and C). Therefore, it appears that c-di-GMP inhibits, primarily or exclusively, Clp binding to PA, the lower affinity site.

Finally, we tested relative contributions of the PA and PB sites in HSAF production by mutating each of these sites in the *L. enzymogenes* chromosome. The replacement of the native PA site to a scrambled site, PA_{sm}, in the chromosome resulted in a significant decrease in HSAF biosynthesis gene expression and HSAF production (Figure 4H and I). Similar results were observed when the native PB was replaced with PB_{sm} (Figure 4H and I). Replacements of both chromosomal sites in combination also significantly decreased *lafB* expression and HSAF production (Figure 4H and I). Taken together, these data establish that both sites are required for Clp-mediated activation of HSAF gene expression and that c-di-GMP-mediated inhibition of Clp binding to the lower-affinity, PA, site may be sufficient to decrease HSAF biosynthesis gene expression.

LchP interacts with Clp

In this part of the study, we investigated the relationship between LchP and Clp. The observation that the *lchP* deletion resulted in a modest increase in intracellular c-di-GMP levels (Figure 3C) poorly correlated with the high impact of LchP on *lafB* gene expression and HSAF production (Figure 3A and B). One possibility that could explain the 'oversized' effect of LchP on Clp was that these proteins interacted directly.

First, we explored this hypothesis at the genetic level. We generated a *clp lchP* double mutant (Δ*clp* Δ*lchP*). As expected, it was impaired in HSAF production (Figure 5A), similar to the Δ*clp* mutant reported in our earlier study (37). Introduction of the plasmid-borne *clp* gene, but not the *lchP* gene, partially restored HSAF production (Figure 5A) likely due to higher than physiological levels of the plasmid-encoded *clp* (Supplementary Figure S7A), sufficient to partially overcome c-di-GMP-dependent inhibition of DNA binding. These data suggest that Clp acts downstream of LchP in the regulatory cascade or, alternatively, that LchP affects Clp protein abundance. We tested the latter possibility by measuring Clp protein levels in the wild type and *lchP* mutant. We observed slightly lower Clp levels in the mutant (Supplementary Figure S7B), which could not account for the strong effect of LchP on Clp-dependent HSAF biosynthesis gene expression.

Next, we asked whether Clp can bind LchP directly. To detect protein-protein interaction, we used a bacterial two-hybrid (B2H) system. As shown in Figure 5B, Clp interacts with LchP-PGE almost as strongly as the positive control provided with the B2H system. In a second assay, we tested the ability of LchP-PGE-MBP to pull down Clp-GST, and observed a positive signal (Figure 5C). The LchP-Clp interaction was further confirmed by the MST experiment, in which LchP-PGE was found to bind to Clp-GST with high affinity (K_d, 1.42 nM) (Figure 5D). Results of these three assays strongly support the notion that the cytoplasmic fragment of LchP physically interacts with Clp. Addition of 16 μM c-di-GMP resulted in a ∼5-fold lower affinity (K_d, 7.18 nM) of LchP-PGE to Clp-GST (Figure 5E), suggesting that c-di-GMP inhibits LchP-Clp interactions.

We further investigated which domains of LchP-PGE are involved in Clp binding. Using the B2H system, we found that both the GGDEF and EAL domains likely contribute

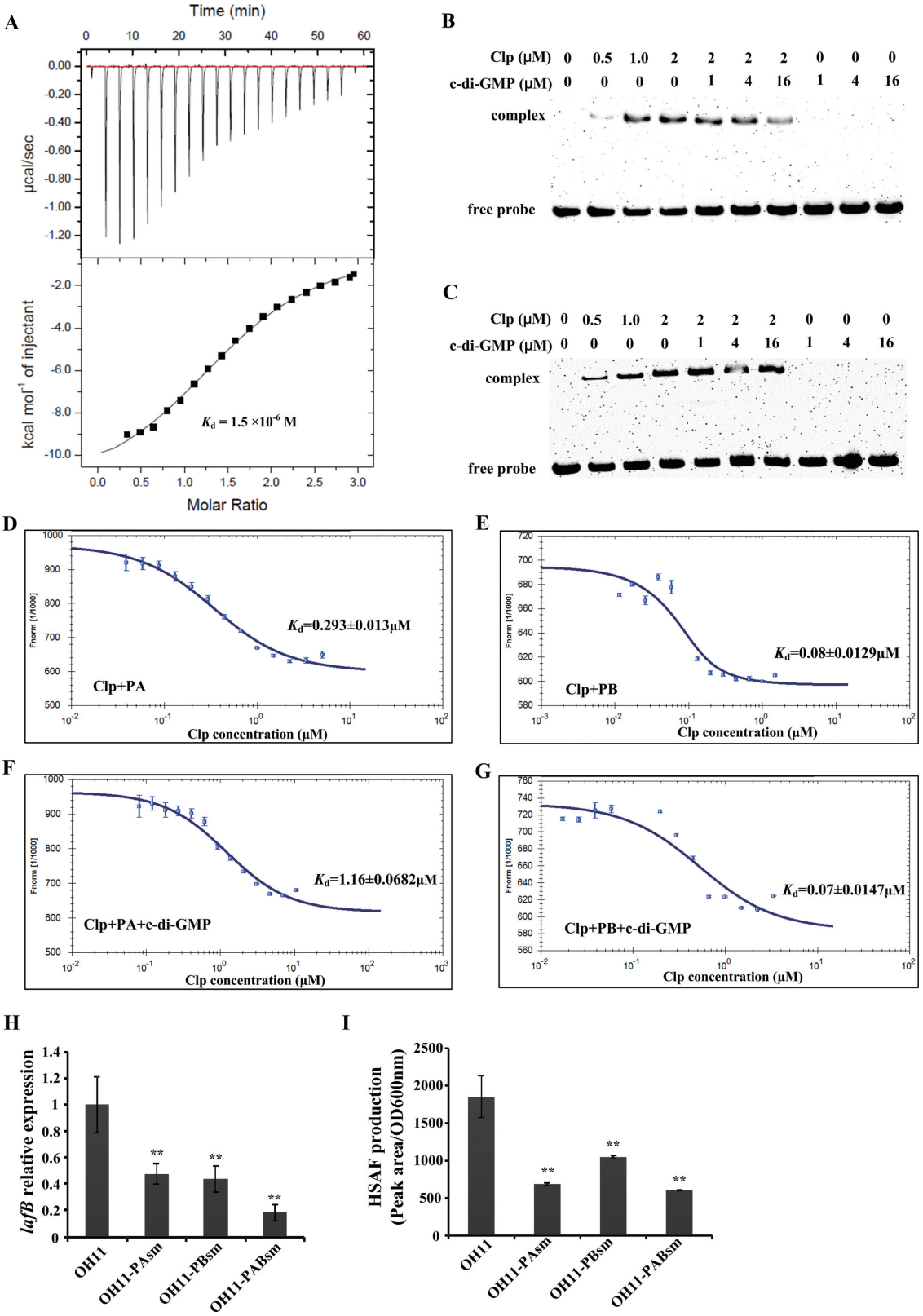

Figure 4. Characterization of Clp binding to the HSAF operon promoter in the presence and absence of c-di-GMP *in vitro* and *in vivo*. (**A**) Characterization of the Clp-c-di-GMP binding via ITC. The K_d of binding is 1.5 μM. (**B** and **C**) EMSA experiments assessing the effect of c-di-GMP on Clp binding to the PA (upstream) (B) and PB (downstream) (C) binding sites within the HSAF operon promoter region. (**D**–**G**) Characterization of the Clp binding affinity via MST. Clp binding to PA in the absence (D) and presence (F) of c-di-GMP. Clp binding affinity to PB in the absence (E) and presence (G) of c-di-GMP. (**H**, **I**) *In vivo* contributions of the PA and PB sites to HSAF production. Replacements of either the PA or PB binding sites by the scrambled sequence sites, PA_{sm} or PB_{sm}, or in combination (PAB_{sm}) significantly lowers transcription of *lafB*, the first gene in the HSAF biosynthesis operon (H) as well as HSAF production (I). Data from three experiments, ±SD. $^{**}P < 0.01$, relative to the wild type.

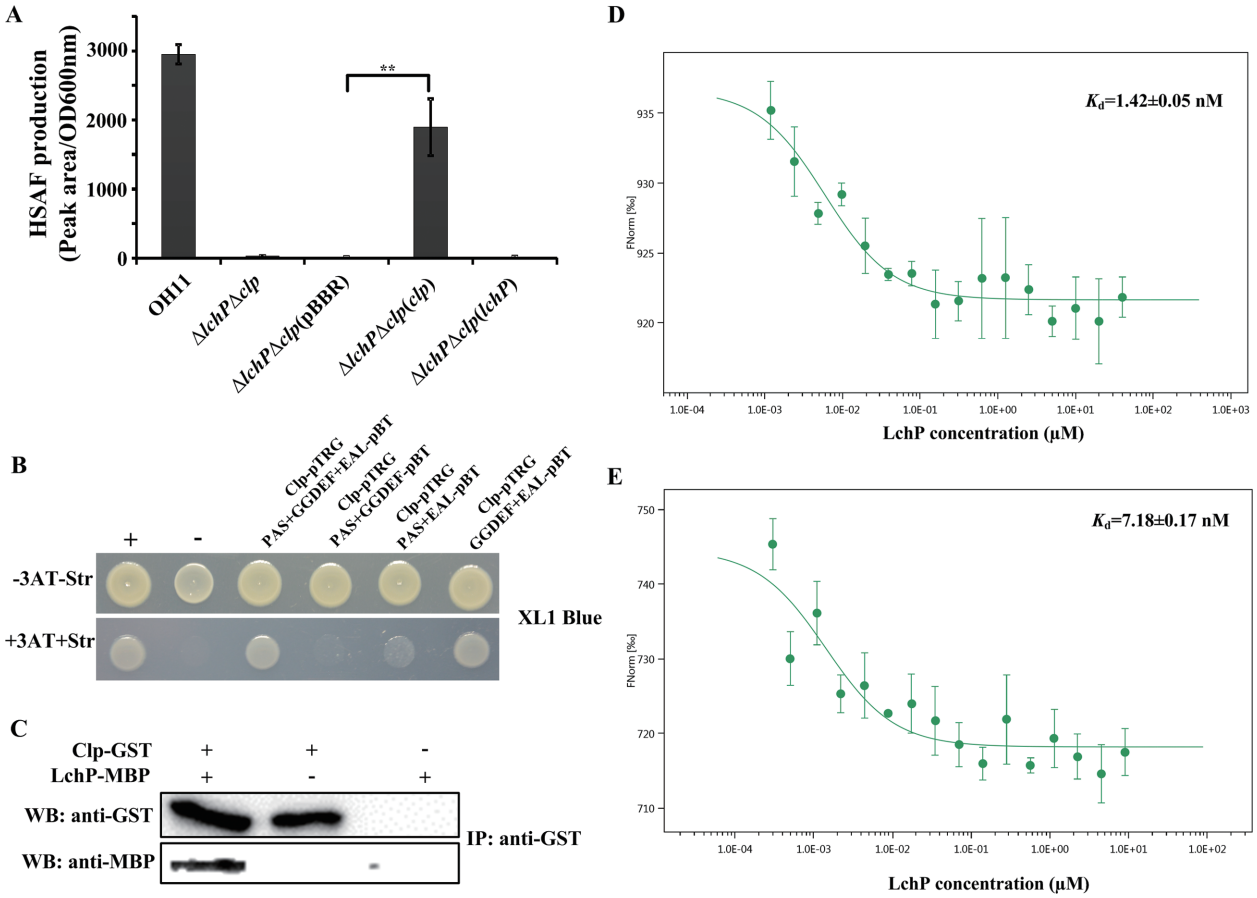

Figure 5. LchP interaction with Clp, the c-di-GMP-binding transcription factor. (**A**) A genetic assay showing that Clp acts downstream of LchP in the pathway regulating HSAF biosynthesis. pBBR, empty vector. Data from three experiments, ±SD. $^{**}P < 0.01$. (**B**) An *E. coli*-based B2H assay showing that both GGDEF and EAL domains are important for physical interactions of the cytoplasmic part of LchP (PAS+GGDEF+EAL) with Clp. +, positive control (GacS-pBT and GacS-pTRG); -, negative control (vectors pBT and pTRG). (**C**) A pull-down assay confirming interactions between Clp and the cytoplasmic fragment of LchP. The IP assay was carried out using anti-GST antibody. The Western blot was performed by using anti-GST and anti-MBP antibodies. (**D**) MST showing that LchP-PGE-MBP forms a complex with Clp-GST with K_d, 1.42 nM. (**E**) MST showing that c-di-GMP lowers affinity of LchP-PGE-MBP to Clp-GST (K_d, 7.18 nM).

to these interactions, whereas the PAS domain is not involved (Figure 5B). The mutations in the conserved EAL and GGDEF motifs, either individually or in combination, had no influence on LchP-PGE–Clp interactions (Supplementary Figure S8).

Finally, to explore how specific the LchP-Clp interaction is, we tested another PDE involved in control of HSAF production, RpfG. No RpfG–Clp binding was detected in the pull-down and MST assays (Supplementary Figure S9), suggesting that the LchP–Clp interaction is specific.

Interactions with Clp enhance PDE activity of LchP

We wondered whether LchP-Clp interactions affect PDE activity of LchP. To test this possibility, we used a biochemical assay where c-di-GMP hydrolysis by LchP-PGE-MBP was assayed in the presence or absence of Clp. The results of the assay showed that PDE activity of LchP-PGE-MBP was higher in the presence, versus absence, of Clp-GST (Figure 6A). As expected, Clp had no effect on c-di-GMP hydrolysis by the inactive LchP-PGE-MBP that contains the mutant AAA motif in place of EAL (Supplementary Figure S10).

To verify the stimulatory effect of Clp on LchP PDE activity by an alternative approach, we used a genetic assay in *E. coli* MG1655 Δ*yhjH*. As shown in Figure 6B and Supplementary Figure S11, swim zones of MG1655 Δ*yhjH* were largest when both LchP-PGE (expressed from pET30a) and Clp (expressed from pBAD) were expressed (Supplementary Figure S12), i.e. in the presence of the *clp* expression inducer, arabinose. In the absence of arabinose (no *clp* expression), the swim zones were smaller. Similar to the biochemical PDE assay, the inactivation of the conserved EAL motif, impaired PDE activity of LchP (Figure 6B and Supplementary Figure S11). Therefore, results of both assays suggest that Clp binding enhances PDE activity of LchP-PGE.

DISCUSSION

In this study, we investigated c-di-GMP-dependent regulation of the antibiotic HSAF biosynthesis in *L. enzymogenes*, an environmental bacterium with significant potential as a biological control agent for fungal diseases of agriculturally important plants. We characterized new components

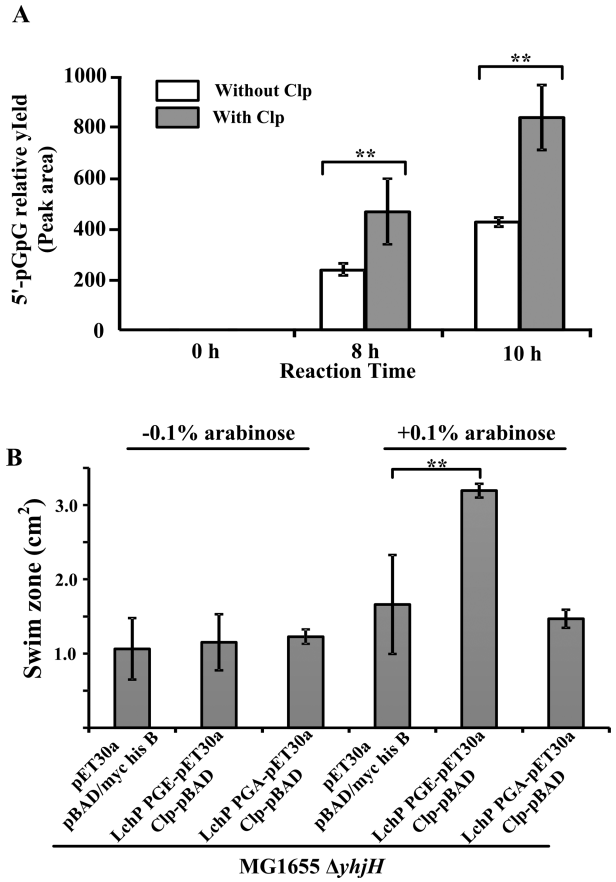

Figure 6. Stimulation of PDE activity of LchP by Clp. (**A**) Increased c-di-GMP hydrolysis by LchP-PGE in the presence of Clp *in vitro*. pGpG was measured by HPLC. Data from three experiments are shown. $^{**}P < 0.01$. (**B**) Increased swim zones in semi-solid agar in strain MG1655 Δ*yhjH* expressing LchP and Clp. LchP-PGE (pET30a-PGE) is expressed constitutively. Clp (pBAD-Clp) is expressed from an arabinose-inducible promoter in the absence or presence of arabinose. Data from three experiments, ±SD are shown. LchP-PGA is the same as LchP-PGE except the 'EAL' motif is mutated to 'AAA'. $^{**}P < 0.01$. The transcription levels of *lchP* and *clp* were confirmed by RT PCR (Supplementary Figure S12).

involved in this regulation, the c-di-GMP-dependent transcription factor, Clp, and the weak c-di-GMP PDE, LchP, that plays a disproportionately large role in HSAF biosynthesis. Clp acts as a major activator that binds to two sites upstream of *lafB*, the first gene in the HSAF biosynthesis operon. It is peculiar that c-di-GMP inhibition of Clp binding to DNA is profound at the lower affinity site but undetectable in our assays at the higher affinity site. Because chromosomal site mutations have shown that both Clp binding sites are important for HSAF operon expression, lower binding to a single site must be sufficient to decrease gene expression.

We identified a c-di-GMP PDE, LchP, as the second PDE, in addition to the previously characterized RpfG, that plays a major role in c-di-GMP-dependent HSAF biosynthesis (26,37). We were surprised that the *lchP* gene deletion resulted in only modest increase in intracellular c-di-GMP concentrations. Our analysis revealed that LchP has low PDE activity, which is at odds with its large effect on HSAF production. These observations prompted our testing for possible LchP–Clp interactions. Not only did we detect such interactions, we found that Clp binding enhances PDE activity of LchP. Thus, the LchP–Clp interactions not only improve the specificity of LchP signaling, but also increase LchP potency (Figure 7).

It is noteworthy that while LchP interacts with Clp specifically, RpfG does not. Therefore, at least two kinds of PDEs responsible for c-di-GMP-dependent suppression of HSAF biosynthesis co-exist in *L. enzymogenes* – RpfG, which can be considered as generic PDE, and LchP, a Clp-specific PDE. We know that PDE activity of RpfG depends on bacterial cell density and is mediated through the quorum sensing molecule, Diffusible Signal Factor (DSF) (47). At this point, we do not know what signals control PDE activity of LchP. We can only speculate that these signals affect LchP activity via the periplasmic sensory domain Reg_prop linked to the Y-Y-Y domain, predicted to be involved in sensing of unsaturated disaccharides (48), and possibly also via the cytoplasmic PAS domains, whose ligands are currently unknown (Figure 7).

A complex between a c-di-GMP binding ribosomal modifying enzyme, RimK, and a PDE, RimA, has been observed in *Pseudomonas fluorescens* (49). However, to our knowledge, this is the first report of a complex between a PDE and a c-di-GMP-binding transcription factor. These examples support the notion that DGCs and PDEs form complexes with their target c-di-GMP-binding proteins, which dates back to the work of Dr. Moshe Benziman, who discovered c-di-GMP in *Acetobacter xylinum* (1), now known as *Komagataeibacter xylinus*. This notion is derived from the observation that the DGCs and PDEs that control activity of the cellulose synthase BcsAB, the first described c-di-GMP-dependent effector protein, were copurified (36,50). Similar complex arrangement has been described in *E. coli* for the DGC DgcO (DosC), its partner PDE PdeO (DosP) (44) and their specific target, the RNA degrading enzyme PNPase (51,52); however, PNPase does not bind c-di-GMP (53). The PDE PdeR (YciR) and the DGC DgcM (YdaM) from *E. coli* form a complex with the transcription factor MlrA, which prevents MlrA from functioning as a transcription activator. MlrA does not bind c-di-GMP but it dissociates from the complex at high c-di-GMP concentrations, which are sensed by the 'trigger' PDE PdeR (54,55). Yet another *E. coli* DGC DgcN (YfiN) localizes to the cell division Z-ring, where it binds to FtsZ and ZipA proteins and inhibits cell division (56). Further, in *P. aeruginosa*, the DGC GcbC interact with the c-di-GMP-binding effector LapD that belongs to the class of degenerate EAL domain proteins capable of c-di-GMP binding (57). The number of examples of complexes formed by the enzymes involved in c-di-GMP synthesis and/or hydrolysis and downstream c-di-GMP-binding effectors continues to grow, and so does the diversity of architectures of such complexes. This leads us to conclude that association of DGCs and PDEs with their downstream effectors is a common mechanism enabling specificity of signaling through the ubiquitous second messenger, c-di-GMP. Consistent with this assessment is the large number of examples in the literature where deletion of individual DGC genes results in very specific phenotypes that do not affect other known c-di-GMP-dependent processes. A striking example

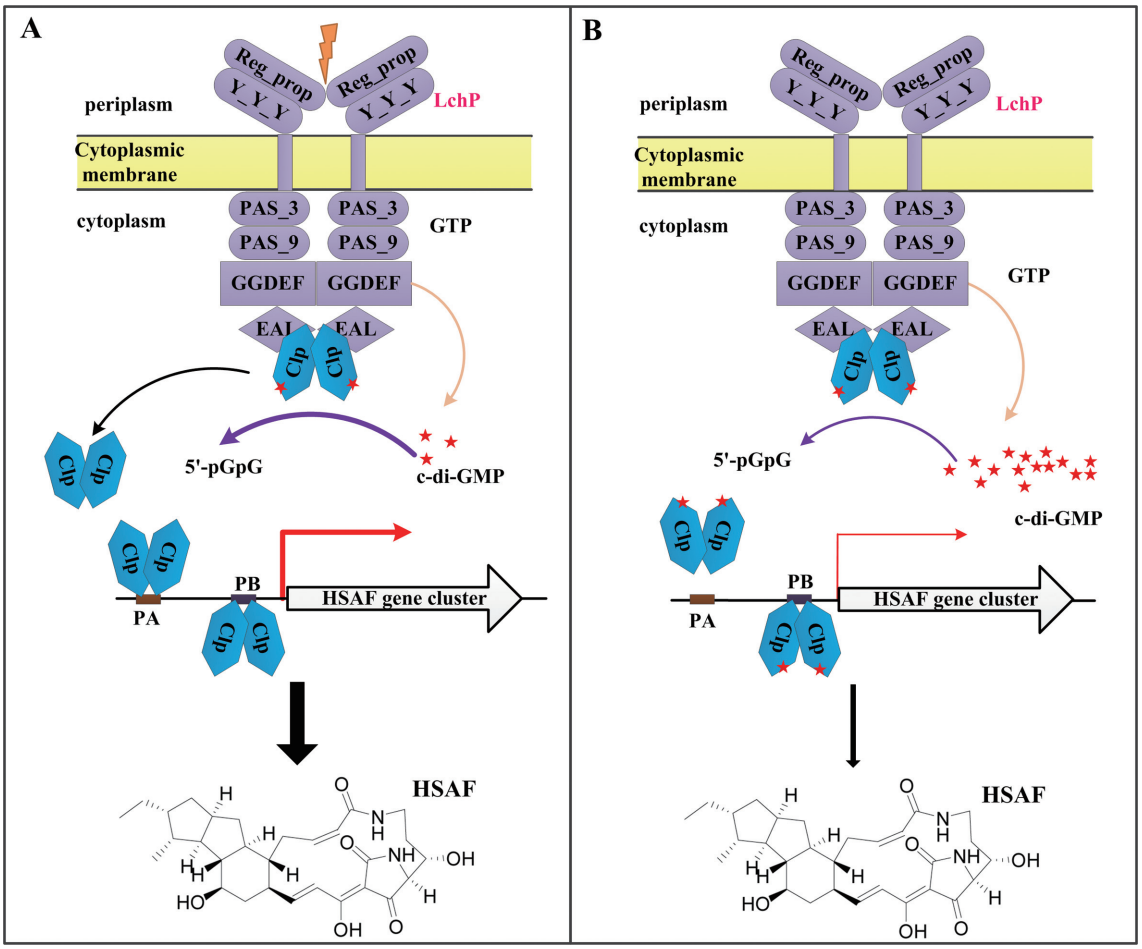

Figure 7. Model of c-di-GMP-dependent regulation of HSAF biosynthesis in *L. enzymogenes*. (**A**) When LchP is activated via as yet unknown factors (orange lightening symbol), it actively degrades c-di-GMP from the Clp-c-di-GMP complex, which leads the release of Clp and activation of the HSAF biosynthesis operon (thick red arrow). The Clp-LchP interaction increases PDE activity of LchP, providing a positive feedback. (**B**) In the absence of signals activating PDE activity of LchP and/or presence of stimuli that increase cellular c-di-GMP levels, the interaction of LchP-Clp and the binding of Clp to the HSAF biosynthesis promoter region are decreased, which leads to lower HSAF biosynthesis operon expression (thin red arrow). The most sensitive to the rise in c-di-GMP is the lower affinity PA site.

of DGC specificity has been observed in *Bdellovibrio bacteriovorus*, where knockout mutants in each of its three DGCs had very distinct, non-overlapping phenotypes (58).

In the cAMP- and cGMP-signaling complexes of eukaryotes, the cAMP/cGMP-binding effector proteins are commonly associated with nucleotide cyclases and/or phosphodiesterases (59). Bacteria seem to follow suit, or more likely, they were first to invent signaling complexes to ensure specificity in second messenger-mediated signaling. Bacteriologists, on the other hand, are just beginning to appreciate these mechanisms, following suit of the researchers studying signal transduction in eukaryotes.

DATA AVAILABILITY

The sequence data of the present study have been submitted to the NCBI Genbank under the following accession numbers: MG387210.1 (Le1632), MG387192.1 (Le0155), MG387193.1 (Le2762/LchP), MG387195.1 (Le3747), MG387194.1 (Le3677), MG387196.1 (Le3882), MG387213.1 (Le4875), MG387215.1 (Le4727/RpfG).

SUPPLEMENTARY DATA

Supplementary Data are available at NAR Online.

ACKNOWLEDGEMENTS

We thank Dr Wei Qian for providing facilities in MST assay and the anti-Clp antibody. We also thank Professor Zheng Qing Fu (University of South Carolina, USA) for discussion and suggestions.
Author Contributions: G.Q. and F.L. conceived the project. G.Q., S.C., M.G. and F.L. designed experiments. G.X., S.H., C.H., K.C., Y.H. carried out experiments. G.X., G.Q., S.C., M.G. and F.L. analyzed data and prepared figures and tables. G.Q. wrote the manuscript draft. S.C., M.G. and F.L. revised the manuscript. All authors read and approved the submission for publication.

FUNDING

National Natural Science Foundation of China [31572046 and 31872046 to G.Q.]; National Basic Research (973) Pro-

gram of China [2015CB150600 to G.Q.]; Fundamental Research Funds for the Central Universities [Y0201600126 and KYTZ201403 to G.Q.]; Innovation Team Program for Jiangsu Universities (2017 to G.Q.); Special Fund for Agro-Scientific Research in the Public Interest [201303015 to G.Q. and F.L.]; National Key Research and Development Program, China [2017YFD0201100 to G.Q. and F.L.]; Jiangsu Provincial Key Technology Support Program [BE2015354 to F.L.]; Basal Research Funds from JAAS [ZX(15)1006 to F.L.]; Jiangsu Agricultural Science and Technology Innovation Funds [CX(16)1049 to F.L.]; '948' Project of the Ministry of Agriculture, China [2014-Z24 to F.L.]; National Pear Industry Technology System [CARS-28-16 to F.L.]; Shan-Ho Chou was supported by the MoST grant of Taiwan [105-2113-M-005-013-MY2]; Mark Gomelsky was supported by US National Institutes of Health [R21 AI135683-01]. Funding for open access charge: National Natural Science Foundation of China.

Conflict of interest statement. None declared.

REFERENCES

1. Ross,P., Weinhouse,H., Aloni,Y., Michaeli,D., Weinberger-Ohana,P., Mayer,R., Braun,S., de Vroom,E., van der Marel,G.A., van Boom,J.H. *et al.* (1987) Regulation of cellulose synthesis in *Acetobacter xylinum* by cyclic diguanylic acid. *Nature*, **325**, 279–281.
2. Romling,U., Galperin,M.Y. and Gomelsky,M. (2013) Cyclic di-GMP: the first 25 years of a universal bacterial second messenger. *Microbiol. Mol. Biol. Rev.*, **77**, 1–52.
3. Jenal,U., Reinders,A. and Lori,C. (2017) Cyclic di-GMP: second messenger extraordinaire. *Nat. Rev. Microbiol.*, **15**, 271–284.
4. Paul,R., Weiser,S., Amiot,N.C., Chan,C., Schirmer,T., Giese,B. and Jenal,U. (2004) Cell cycle-dependent dynamic localization of a bacterial response regulator with a novel di-guanylate cyclase output domain. *Genes Dev.*, **18**, 715–727.
5. Ryjenkov,D.A., Tarutina,M., Moskvin,O.V. and Gomelsky,M. (2005) Cyclic diguanylate is a ubiquitous signaling molecule in bacteria: Insights into biochemistry of the GGDEF protein domain. *J. Bacteriol.*, **187**, 1792–1798.
6. Schmidt,A.J., Ryjenkov,D.A. and Gomelsky,M. (2005) The ubiquitous protein domain EAL is a cyclic diguanylate-specific phosphodiesterase: enzymatically active and inactive EAL domains. *J. Bacteriol.*, **187**, 4774–4781.
7. Christen,M., Christen,B., Folcher,M., Schauerte,A. and Jenal,U. (2005) Identification and characterization of a cyclic di-GMP-specific phosphodiesterase and its allosteric control by GTP. *J. Biol. Chem.*, **280**, 30829–30837.
8. Tamayo,R., Tischler,A.D. and Camilli,A. (2005) The EAL domain protein VieA is a cyclic diguanylate phosphodiesterase. *J. Biol. Chem.*, **280**, 33324–33330.
9. Bellini,D., Caly,D.L., McCarthy,Y., Bumann,M., An,S.Q., Dow,J.M., Ryan,R.P. and Walsh,M.A. (2014) Crystal structure of an HD-GYP domain cyclic-di-GMP phosphodiesterase reveals an enzyme with a novel trinuclear catalytic iron centre. *Mol. Microbiol.*, **91**, 26–38.
10. Römling,U., Gomelsky,M. and Galperin,M.Y. (2005) c-di-GMP: the dawning of a novel bacterial signaling system. *Mol. Microbiol.*, **57**, 629–639.
11. Li,S., Du,L., Yuen,G. and Harris,S.D. (2006) Distinct ceramide synthases regulate polarized growth in the filamentous fungus *Aspergillus nidulans*. *Mol. Biol. Cell*, **17**, 1218–1227.
12. Yu,F., Zaleta-Rivera,K., Zhu,X., Huffman,J., Millet,J.C., Harris,S.D., Yuen,G., Li,X.C. and Du,L. (2007) Structure and biosynthesis of heat-stable antifungal factor (HSAF), a broad-spectrum antimycotic with a novel mode of action. *Antimicrob. Agents Chemother.*, **51**, 64–72.
13. Lou,L.L., Qian,G.L., Xie,Y.X., Hang,J.L., Chen,H.T., Zaleta-Riyera,K., Li,Y.Y., Shen,Y.M., Dussault,P.H., Liu,F.Q. *et al.* (2011) Biosynthesis of HSAF, a tetramic acid-containing macrolactam from *Lysobacter enzymogenes*. *J. Am. Chem. Soc.*, **133**, 643–645.
14. Xu,L., Wu,P., Wright,S.J., Du,L. and Wei,X. (2015) Bioactive polycyclic tetramate macrolactams from *Lysobacter enzymogenes* and their absolute configurations by theoretical ECD calculations. *J. Nat. Prod.*, **78**, 1841–1847.
15. Li,S., Jochum,C.C., Yu,F., Zaleta-Rivera,K., Du,L., Harris,S.D. and Yuen,G.Y. (2008) An antibiotic complex from *Lysobacter enzymogenes* strain C3: antimicrobial activity and role in plant disease control. *Phytopathology*, **98**, 695–701.
16. Su,Z., Chen,H., Wang,P., Tombosa,S., Du,L., Han,Y., Shen,Y., Qian,G. and Liu,F. (2017) 4-Hydroxybenzoic acid is a diffusible factor that connects metabolic shikimate pathway to the biosynthesis of a unique antifungal metabolite in *Lysobacter enzymogenes*. *Mol. Microbiol.*, **104**, 163–178.
17. Wang,P., Chen,H., Qian,G. and Liu,F. (2017) LetR is a TetR family transcription factor from *Lysobacter* controlling antifungal antibiotic biosynthesis. *Appl. Microbiol. Biotechnol.*, **101**, 3273–3282.
18. Chen,Y., Xia,J., Su,Z., Xu,G., Gomelsky,M., Qian,G. and Liu,F. (2017) The regulator of type IV pili synthesis, PilR, from *Lysobacter* controls antifungal antibiotic production via a c-di-GMP pathway. *Appl. Environ. Microbiol.*, **83**, e03397-16.
19. Liang,Z. X. (2015) The expanding roles of c-di-GMP in the biosynthesis of exopolysaccharides and secondary metabolites. *Nat. Prod. Rep.*, **32**, 663–683.
20. Fineran,P.C., Williamson,N.R., Lilley,K.S. and Salmond,G.P. (2007) Virulence and prodigiosin antibiotic biosynthesis in *Serratia* are regulated pleiotropically by the GGDEF/EAL domain protein, PigX. *J. Bacteriol.*, **189**, 7653–7662.
21. Tschowri,N. (2016) Cyclic dinucleotide-controlled regulatory pathways in *Streptomyces* species. *J. Bacteriol.*, **198**, 47–54.
22. Chng,C., Lum,A.M., Vroom,J.A. and Kao,C.M. (2008) A key developmental regulator controls the synthesis of the antibiotic erythromycin in *Saccharopolyspora erythraea*. *Proc. Natl. Acad. Sci. U.S.A.*, **105**, 11346–11351.
23. Malone,J.G., Jaeger,T., Spangler,C., Ritz,D., Spang,A., Arrieumerlou,C., Kaever,V., Landmann,R. and Jenal,U. (2010) YfiBNR mediates cyclic di-GMP dependent small colony variant formation and persistence in *Pseudomonas aeruginosa*. *PLoS Pathog*, **6**, e1000804.
24. D'Alvise,P.W., Magdenoska,O., Melchiorsen,J., Nielsen,K.F. and Gram,L. (2014) Biofilm formation and antibiotic production in *Ruegeria mobilis* are influenced by intracellular concentrations of cyclic dimeric guanosinmonophosphate. *Environ. Microbiol.*, **16**, 1252–1266.
25. Qian,G.L., Wang,Y.L., Liu,Y.R., Xu,F.F., He,Y.W., Du,L.C., Venturi,V., Fan,J.Q., Hu,B.S. and Liu,F.Q. (2013) *Lysobacter enzymogenes* uses two distinct cell-cell signaling systems for differential regulation of secondary-metabolite biosynthesis and colony morphology. *Appl. Environ. Microbiol.*, **79**, 6604–6616.
26. Han,Y., Wang,Y., Tombosa,S., Wright,S., Huffman,J., Yuen,G., Qian,G.L., Liu,F.Q., Shen,Y.M. and Du,L.C. (2015) Identification of a small molecule signaling factor that regulates the biosynthesis of the antifungal polycyclic tetramate macrolactam HSAF in *Lysobacter enzymogenes*. *Appl. Microbiol. Biotechnol.*, **99**, 801–811.
27. Leduc,J.L. and Roberts,G.P. (2009) Cyclic di-GMP allosterically inhibits the CRP-like protein (Clp) of *Xanthomonas axonopodis* pv. *citri*. *J. Bacteriol.*, **191**, 7121–7122.
28. Chin,K.H., Lee,Y.C., Tu,Z.L., Chen,C.H., Tseng,Y.H., Yang,J.M., Ryan,R.P., McCarthy,Y., Dow,J.M., Wang,A.H.J. *et al.* (2010) The cAMP receptor-like protein CLP is a novel c-di-GMP receptor linking cell-cell Signaling to virulence gene expression in *Xanthomonas campestris*. *J. Mol. Biol.*, **396**, 646–662.
29. Tao,F., He,Y.W., Wu,D.H., Swarup,S. and Zhang,L.H. (2010) The cyclic nucleotide monophosphate domain of *Xanthomonas campestris* global regulator Clp defines a new class of cyclic di-GMP effectors. *J. Bacteriol.*, **192**, 1020–1029.
30. Finn,R.D., Coggill,P., Eberhardt,R.Y., Eddy,S.R., Mistry,J., Mitchell,A.L., Potter,S.C., Punta,M., Qureshi,M., Sangrador-Vegas,A. *et al.* (2016) The Pfam protein families database: towards a more sustainable future. *Nucleic Acids Res.*, **44**, D279–D285.
31. Finn,R.D., Clements,J. and Eddy,S.R. (2011) HMMER web server: interactive sequence similarity searching. *Nucleic Acids Res.*, **39**, W29–W37.

32. Qian,G.L., Wang,Y.S., Qian,D.Y., Fan,J.Q., Hu,B.S. and Liu,F.Q. (2012) Selection of available suicide vectors for gene mutagenesis using *chiA* (a chitinase encoding gene) as a new reporter and primary functional analysis of *chiA* in *Lysobacter enzymogenes* strain OH11. *World J. Microb. Biotechnol.*, **28**, 549–557.
33. Qian,G.L., Xu,F.F., Venturi,V., Du,L.C. and Liu,F.Q. (2014) Roles of a solo LuxR in the biological control agent *Lysobacter enzymogenes* strain OH11. *Phytopathology*, **104**, 224–231.
34. Livak,K.J. and Schmittgen,T.D. (2001) Analysis of relative gene expression data using Real-Time Quantitative PCR and the $2^{-\Delta\Delta CT}$ method. *Methods*, **25**, 402–408.
35. Ryu,M.H., Fomicheva,A., O'Neal,L., Alexandre,G. and Gomelsky,M. (2017) Using light-activated enzymes for modulating intracellular c-di-GMP levels in bacteria. *Methods Mol. Biol.*, **1657**, 169–186.
36. Ryjenkov,D.A., Simm,R., Römling,U. and Gomelsky,M. (2006) The PilZ domain is a receptor for the second messenger c-di-GMP. The PilZ domain protein YcgR controls motility in enterobacteria. *J. Biol. Chem.*, **281**, 30310–30314.
37. Wang,Y.S., Zhao,Y.X., Zhang,J., Zhao,Y.Y., Shen,Y., Su,Z.H., Xu,G.G., Du,L.C., Huffman,J.M., Venturi,V. *et al.* (2014) Transcriptomic analysis reveals new regulatory roles of Clp signaling in secondary metabolite biosynthesis and surface motility in *Lysobacter enzymogenes* OH11. *Appl. Microbiol. Biotechnol.*, **98**, 9009–9020.
38. Goodman,A.L., Merighi,M., Hyodo,M., Ventre,I., Filloux,A. and Lory,S. (2009) Direct interaction between sensor kinase proteins mediates acute and chronic disease phenotypes in a bacterial pathogen. *Gene Dev.*, **23**, 249–259.
39. Xu,H., Chen,H., Shen,Y., Du,L., Chou,S.H., Liu,H., Qian,G. and Liu,F. (2016) Direct regulation of extracellular chitinase production by the transcription factor LeClp in *Lysobacter enzymogenes* OH11. *Phytopathology*, **106**, 971–977.
40. Hickman,J.W. and Harwood,C.S. (2008) Identification of FleQ from *Pseudomonas aeruginosa* as a c-di-GMP-responsive transcription factor. *Mol. Microbiol.*, **69**, 376–389.
41. Zhu,B., Liu,C., Liu,S., Cong,H., Chen,Y., Gu,L. and Ma,L.Z. (2016) Membrane association of SadC enhances its diguanylate cyclase activity to control exopolysaccharides synthesis and biofilm formation in *Pseudomonas aeruginosa*. *Environ. Microbiol.*, **18**, 3440–3452.
42. Thormann,K.M., Duttler,S., Saville,R.M., Hyodo,M., Shukla,S., Hayakawa,Y. and Spormann,A.M. (2006) Control of formation and cellular detachment from *Shewanella oneidensis* MR-1 biofilms by cyclic di-GMP. *J. Bacteriol.*, **188**, 2681–2691.
43. Boehm,A., Kaiser,M., Li,H., Spangler,C., Kasper,C.A., Ackermann,M., Kaever,V., Sourjik,V., Roth,V. and Jenal,U. (2010) Second messenger-mediated adjustment of bacterial swimming velocity. *Cell*, **141**, 107–116.
44. Hengge,R., Galperin,M.Y., Ghigo,J.M., Gomelsky,M., Green,J., Hughes,K.T., Jenal,U. and Landini,P. (2016) Systematic nomenclature for GGDEF and EAL domain-containing c-di-GMP turnover proteins of *Escherichia coli*. *J. Bacteriol.*, **198**, 7–11.
45. Zhou,L., Wang,X.Y., Sun,S., Yang,L.C., Jiang,B.L. and He,Y.W. (2015) Identification and characterization of naturally occurring DSF-family quorum sensing signal turnover system in the phytopathogen *Xanthomonas*. *Environ. Microbiol.*, **17**, 4646–4658.
46. Baaske,P., Wienken,C.J., Reineck,P., Duhr,S. and Braun,D. (2010) Optical thermophoresis for quantifying the buffer dependence of aptamer binding. *Angew. Chem.*, **49**, 2238–2241.
47. Deng,Y., Schmid,N., Wang,C., Wang,J., Pessi,G., Wu,D., Lee,J., Aguilar,C., Ahrens,C.H., Chang,C. *et al.* (2012) Cis-2-dodecenoic acid receptor RpfR links quorum-sensing signal perception with regulation of virulence through cyclic dimeric guanosine monophosphate turnover. *Proc. Natl. Acad. Sci. U.S.A.*, **109**, 15479–15484.
48. Lowe,E.C., Basle,A., Czjzek,M., Firbank,S.J. and Bolam,D.N. (2012) A scissor blade-like closing mechanism implicated in transmembrane signaling in a Bacteroides hybrid two-component system. *Proc. Natl. Acad. Sci. U.S.A.*, **109**, 7298–7303.
49. Little,R.H., Grenga,L., Saalbach,G., Howat,A.M., Pfeilmeier,S., Trampari,E. and Malone,J.G. (2016) Adaptive remodeling of the bacterial proteome by specific ribosomal modification regulates *Pseudomonas* infection and niche colonisation. *PLoS Genet.*, **12**, e1005837.
50. Tal,R., Wong,H.C., Calhoon,R., Gelfand,D., Fear,A.L., Volman,G., Mayer,R., Ross,P., Amikam,D., Weinhouse,H. *et al.* (1998) Three cdg operons control cellular turnover of cyclic di-GMP in Acetobacter xylinum: genetic organization and occurrence of conserved domains in isoenzymes. *J. Bacteriol.*, **180**, 4416–4425.
51. Tuckerman,J.R., Gonzalez,G., Sousa,E.H., Wan,X., Saito,J.A., Alam,M. and Gilles-Gonzalez,M.A. (2009) An oxygen-sensing diguanylate cyclase and phosphodiesterase couple for c-di-GMP control. *Biochemistry*, **48**, 9764–9774.
52. Tuckerman,J.R., Gonzalez,G. and Gilles-Gonzalez,M.A. (2011) Cyclic di-GMP activation of polynucleotide phosphorylase signal-dependent RNA processing. *J Mol Biol.*, **407**, 633–639.
53. Fang,X., Ahmad,I., Blanka,A., Schottkowski,M., Cimdins,A., Galperin,M.Y., Romling,U. and Gomelsky,M. (2014) GIL, a new c-di-GMP-binding protein domain involved in regulation of cellulose synthesis in enterobacteria. *Mol. Microbiol.*, **93**, 439–452.
54. Lindenberg,S., Klauck,G., Pesavento,C., Klauck,E. and Hengge,R. (2013) The EAL domain protein YciR acts as a trigger enzyme in a c-di-GMP signalling cascade in *E. coli* biofilm control. *EMBO J.*,**32**, 2001–2014.
55. Hengge,R. (2016) Trigger phosphodiesterases as a novel class of c-di-GMP effector proteins. *Philos. Trans. R. Soc. Lond. B Biol. Sci.*, **371**, 20150498.
56. Kim,H.K. and Harshey,R.M. (2016) A diguanylate cyclase acts as a cell division inhibitor in a two-step response to reductive and envelope stresses. *mBio*, **7**, e00822-16.
57. Dahlstrom,K.M., Giglio,K.M., Collins,A.J., Sondermann,H. and O'Toole,G.A. (2015) Contribution of physical interactions to signaling specificity between a diguanylate cyclase and its effector. *mBio*, **6**, e01978-15.
58. Hobley,L., Fung,R.K., Lambert,C., Harris,M.A., Dabhi,J.M., King,S.S., Basford,S.M., Uchida,K., Till,R., Ahmad,R. *et al.* (2012) Discrete cyclic di-GMP-dependent control of bacterial predation versus axenic growth in *Bdellovibrio bacteriovorus*. *PLoS Pathog.*, **8**, e1002493.
59. McCormick,K. and Baillie,G.S. (2014) Compartmentalisation of second messenger signaling pathways. *Curr. Opin. Genet. Dev.*, **27**, 20–25.